AUT Journal of Mechanical Engineering

AUT J. Mech. Eng., 2(2) (2018) 137-148
DOI: 10.22060/ajme.2018.13954.5697

Experimental and Numerical Study on the Accuracy of Residual Stress Measurement by Incremental Ring-Core Method

M. A. Moazam, M. Honarpisheh*

Faculty of Mechanical Engineering, University of Kashan, Kashan, Iran

ABSTRACT: In this study, the calibration constants of incremental step method have been determined by finite element analysis to calculate the residual stresses by the ring-core method. The calibration coefficients have been determined by simulation the uniaxial and biaxial loading. It is indicated that the loading approach has not effect on the calibration constants and they are unique. The uniaxial condition has been used to determine the calibration coefficients in the experimental method. To verify the determined constants, the calibration factors have been used to calculate the residual stresses in the case of uniform and non-uniform residual stresses. The axial and biaxial conditions have been studied and the results are in good accordance with applied stresses in simulations. In the uniaxial loading the measured residual stresses in finite element model completely accommodated by the applied stresses and presented formula and calibration constants determined the direction of the maximum principal stress by clearance less than 0.7%. Clearance of the measures stresses and applied stresses in the non-uniform case was about 1 %. An experimental test has been used to show the effectiveness of the obtained calibration coefficient by finite element analysis. Also, it is indicated that the results of the experimental test are satisfactory.

Review History:

Received: 13 January 2018
Revised: 5 May 2018
Accepted: 24 June 2018
Available Online: 15 July 2018

Keywords:

Residual stress
Ring-Core
Calibration coefficients
Incremental method

1- Introduction

In the manufacturing of parts and equipment the residual stresses are important and this topic is considered nowadays. Control the residual stresses in the parts that are subjected to the cyclic loads is serious and in some manufacturing standard measurement the residual stresses are mandatory. For example tension residual stresses on the foot of the rails shall not exceed than 250 MPa [1]. There are many different methods for measuring the residual stresses such as hole-drilling [2, 3], slitting method [4-7], and contour method [8, 9], but each method has its property and could be used just in certain conditions.

Residual stress measurement methods could be classified into three main categories named destructive, semi destructive and non-destructive. Stress could not be measured directly and usually is calculated by measuring the strain. The strains could be measured with electrical strain gages. To determine the residual stresses with strain gage at first the strain gage is bonded on the surface of the specimen, then the equilibrium of the residual stresses are disturbed by material removing process similar machining. As the result new equilibrium condition is made and some deformations will occur. The strain gages sense the strain due to the deformations and by using the appropriate mathematical relation the measured strains are used to measure the residual stresses. Hole-drilling is known as the most famous semi-destructive method which used the strain gage to measure the residual stresses. This method is standardized by ASTM [10]. The ring-core method is another semi-destructive method and based on the same principal as the hole-drilling. The ring-core method allows for determination of residual stresses at high depth from the surface [11]. In ring-core method by cutting an annular groove in stressed specimen, the strains will be relaxed in the core of the ring. It is possible to estimate the residual stresses before cutting the annular groove by use the released strains on the surface of the core [12]. Sensing the stress change inside, the material by the sensor attached at the top of the component is not suitable by using the classic Hook´s law. Thus, there are three commonly used evaluation techniques for residual stress determination: incremental, differential and integral [13]. Each technique has its background and specific mathematical formula and all of them need to calibration coefficients. The calibration coefficients of each technique are unique and they are not related to each other.

Calibration factors in each technique could be determined by experimental test and also by Finite Element (FE) analysis. In the determination of the calibration factors process a known residual stress field should be used. Uniaxial tension and compression field are the best conditions in the uniform case of the residual stresses and bending could be used in non-uniform residual stress distribution along the thickness of the specimen. Marisa and Peterson [14] used the bending condition to make known residual stress distribution. Keil [15] determined the calibration coefficients of incremental technique by using the tension test in a bulk specimen. Václavík et al. [16] used the FE analysis to determine the calibration coefficients, they also measured the residual stresses in a bulk forged shaft by the ring-core method. Civin and Vik [17] used FE model for determination of calibration coefficients and they also proposed a new set of calibration factors.

The ring-core method is relatively common to measure the residual stresses, especially in case of bulk materials similar which manufactured by casting and forging. Although the theory of the ring core method is well-known, but the connection between experimental measurements and

Corresponding author, E–mail: honarpishe@kashanu.ac.ir

numerical studies is still not sufficient. Residual stress measurement by the ring-core method needs to adequate calibration coefficients. There is not still a unique set of calibration constants for each technique of the ring-core method. Final element method is the most effective way to determine the calibration factors. In this research an appropriate numerical model has been studied to determine the calibration factors for the incremental technique of the ring-core method. Also the required formula to determine the calibration constants in the biaxial case have been introduced. Effectiveness of the constants have been studied by simulation the uniform and the non-uniform residual stress fields. The results have been very satisfactory in the case of the both uniform and non-uniform residual stresses. Moreover to the FE analysis an experimental test has been devised to indicate the effectiveness of the calibration constants. The results of the experimental tests are in good accordance with the expected results and conform the FE analysis. Therefore, the presented calibration constants could be used in experimental residual stress measurement by the ring core method as a pre-requested constants. The presented constant improve the final results in comparing with the constants that presented by [15].

2- Principles of Incremental Ring-Core Method

In the ring-core method a small annular groove is made on the surface of the specimen and separates the central core of the surrounding material. This separation causes the release some parts of the residual stresses [15]. This method was innovated by Milberat [18] and modified by several other researchers. During the development of the ring-core method, a special strain rosette was made. This rosette is bonded on the surface of the specimen and the annular groove is made around it. The ring-core rosette is made of three strain gages and each gage is displaced by 45 degrees. Fig. 1 indicates the ring-core method strain rosette.

As mentioned in the previous section, there are three main techniques to calculate the residual stresses by the ring-core method named differential, integral and incremental. By differential method, it is possible to make a rapid test and estimate the value of the residual stresses. This technique could be used as a workshop quality control test. In this technique residual stress are calculated by relieving strains that measured at two different depths and step's difference ΔZ consist of two particular depths Z_i and $2Z_i$, described by Eq. (1). Residual stresses are calculated by Eqs. (2) and (3) [20].

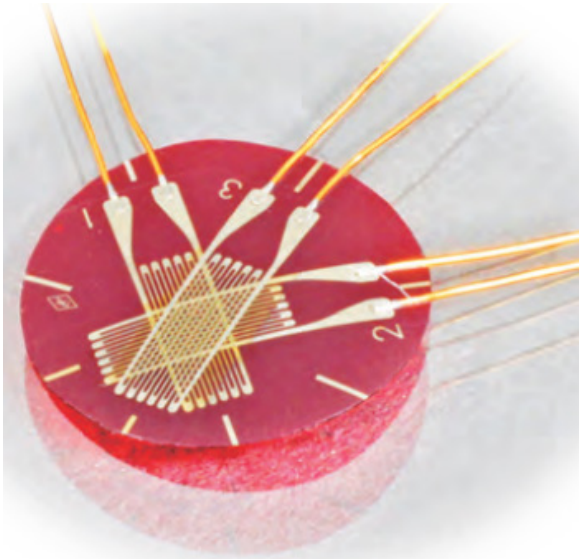

Fig. 1. The ring-core strain rosette [19].

$$\Delta Z = 2Z_i - Z_i = Z_i \qquad Z_i = 1,2,3,\ldots mm \tag{1}$$

$$\sigma_1 = A\,\Delta\varepsilon_1 - B\,\Delta\varepsilon_2 \tag{2}$$

$$\sigma_2 = A\,\Delta\varepsilon_2 - B\,\Delta\varepsilon_1 \tag{3}$$

In Eqs. (2) and (3), A and B are calibration coefficients and σ_1 and σ_2 are principal residual stresses. $\Delta\varepsilon_1$ and $\Delta\varepsilon_2$ are calculated by the Eqs. (4) and (5).

$$\Delta\varepsilon_1 = (\varepsilon_1)_{2Zi} - (\varepsilon_1)_{Zi} \tag{4}$$

$$\Delta\varepsilon_2 = (\varepsilon_2)_{2Zi} - (\varepsilon_2)_{Zi} \tag{5}$$

The integral method commonly used for hole drilling method and its constants described in ASTM E837 standard [10]. Ajovalasit et al. [21] applied integral method to the ring-core. Barsanti et al. [22] determined the constants of integration-method by finite element analysis. The integral method is presented by Eq. (6) and it is assumed that $\varepsilon_x(H)$ relieved on the surface after milling the groove of depth H is the integral of infinitesimal strains due to the residual stresses $\sigma_x(Z)$ acting in whole groove depth [21].

$$\varepsilon_x(H) = \frac{1}{E}\int_0^H F(H,Z)\,\sigma_x(z)\,dz \tag{6}$$

Because this paper deals with the incremental method, it is described in detail. Residual stresses could be uniform or non uniform in plane of measurement and in the depth direction. On the surface of the specimen the plane stress condition exists and this is means that the stress perpendicular to the free surface is zero. Also, it is assumed that in the plane of measurement the magnitude of the residual stresses is constant or its variation is negligible. Thickness of the specimen could be thin of thick, but in the thin case just a uniform case of residual stresses should be considered. Principles of the ring core method and incremental technique is indicated in Fig. 2 [15].

Layer removal, equal to dz, cause to release the residual stresses in this portion of the specimen and cause some deformation in the core. Strain gages will sense the strains on the core surface. If just the strain gage (a) is considered, it is possible to introduce the released strain ε_a on the surface of the core as a function of depth by Eq. (7) [15].

$$\frac{d\,\varepsilon_a(z)}{dz} = K_a(z)\,\epsilon_a^*(z) \tag{7}$$

In Eq. (7), $\epsilon_a^*(z)$ is the measured strain by the strain gage (a) in depth (Z). $K_a(z)$ is the calibration constant related to direction (a) and depth (Z). By considering the uniaxial residual stress condition the Eq. (7) could be written in the form of the Eq. (8).

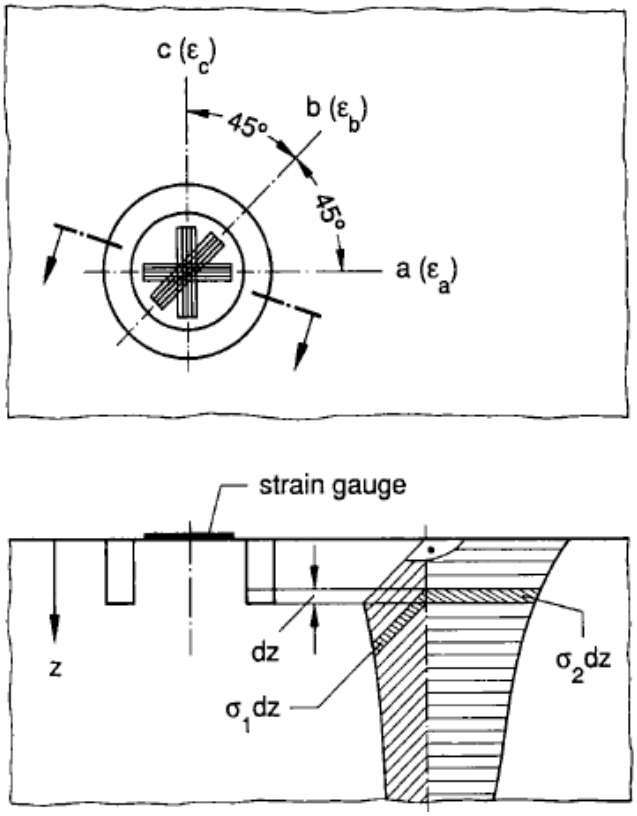

Fig. 2. Used parameters in the incremental ring core method [15].

$$\frac{d\varepsilon_1(z)}{dz} = K_1(z)\frac{1}{E}\sigma_1(z) \tag{8}$$

In Eq. (8), E is the module of elasticity, $K_1(z)$ is the calibration constant related to direction (1) and depth (Z). It is well-known that stress σ_1 makes the strains $\varepsilon_1=(1/E)\sigma_1$ and $\varepsilon_2=(-\nu/E)\sigma_1$. Therefore, it is possible to predict the measured strain by strain-gage2 which is perpendicular to the strain-gage 1, by Eq. (9).

$$\frac{d\varepsilon_2(z)}{dz} = K_2(z)\frac{-\nu}{E}\sigma_1(z) \tag{9}$$

In Eq. (9), $K_2(z)$ is the calibration constant related to direction (2) and depth (Z). By attention to mentioned notes, it is possible to determine the calibration constant by using the known principal direction. To determine the calibration constant $K_1(z)$ and $K_2(z)$ the uniaxial tension test or simulation the uniaxial condition could be considered. The calibration constants have been calculated by Eqs. (8) and (9) and presented by Eqs. (10) and (11).

$$K_1(z) = \frac{E}{\sigma_1}\frac{d\varepsilon_1(z)}{dz} \tag{10}$$

$$K_2(z) = \frac{E}{-\nu\sigma_1}\frac{d\varepsilon_2(z)}{dz} \tag{11}$$

If σ_2 applies in the principal direction (2), then the biaxial condition could be considered. In this condition the effect of σ_2 should superimposed by σ_1. Therefore, the measured strains in principal directions could be presented by Eqs. (12) and (13).

$$\frac{d\varepsilon_1(z)}{dz} = \frac{1}{E}K_1(z)\sigma_1(z) - \frac{\nu}{E}K_2(z)\sigma_2(z) \tag{12}$$

$$\frac{d\varepsilon_2(z)}{dz} = \frac{1}{E}K_1(z)\sigma_2(z) - \frac{\nu}{E}K_2(z)\sigma_1(z) \tag{13}$$

It is possible to determine the magnitude of the principal residual stresses by arranging the Eqs. (12) and (13). Eqs (14) and (15) present the principal residual stresses.

$$\sigma_1(z) = \frac{E}{K_1^{\,2}-\nu^2K_2^{\,2}}\left[K_1(z)\frac{d\varepsilon_1(z)}{dz} + \upsilon K_2(z)\frac{d\varepsilon_2(z)}{dz}\right] \tag{14}$$

$$\sigma_2(z) = \frac{E}{K_1^{\,2}-\nu^2K_2^{\,2}}\left[K_1(z)\frac{d\varepsilon_2(z)}{dz} + \upsilon K_2(z)\frac{d\varepsilon_1(z)}{dz}\right] \tag{15}$$

It is possible to extend the Eqs. (14) and (15) to any two perpendicular system. If “a” perpendicular to “c” and “b” perpendicular to “d” then the Eqs. (16) to (19) are confirmed.

$$\sigma_a(z) = \frac{E}{K_a^{\,2}-\nu^2K_c^{\,2}}\left[K_a(z)\frac{d\varepsilon_a(z)}{dz} + \upsilon K_c(z)\frac{d\varepsilon_c(z)}{dz}\right] \tag{16}$$

$$\sigma_c(z) = \frac{E}{K_a^{\,2}-\nu^2K_c^{\,2}}\left[K_a(z)\frac{d\varepsilon_c(z)}{dz} + \upsilon K_c(z)\frac{d\varepsilon_a(z)}{dz}\right] \tag{17}$$

$$\sigma_b(z) = \frac{E}{K_b^{\,2}-\nu^2K_d^{\,2}}\left[K_b(z)\frac{d\varepsilon_b(z)}{dz} + \upsilon K_d(z)\frac{d\varepsilon_d(z)}{dz}\right] \tag{18}$$

$$\sigma_d(z) = \frac{E}{K_a^{\,2}-\nu^2K_c^{\,2}}\left[K_b(z)\frac{d\varepsilon_d(z)}{dz} + \upsilon K_d(z)\frac{d\varepsilon_b(z)}{dz}\right] \tag{19}$$

From the Mohr’s circle, the Eqs. (20) and (21) are easily verified.

$$\sigma_a + \sigma_c = \sigma_b + \sigma_d = \sigma_1 + \sigma_2 \tag{20}$$

$$d\varepsilon_a + d\varepsilon_c = d\varepsilon_b + d\varepsilon_d = d\varepsilon_1 + d\varepsilon_2 \tag{21}$$

By substituting the Eqs. (20) and (21) to the Eqs. (16) to (19), the Eqs. (22) and (23) will be created.

$$K_a(z) = K_b(z) = K_1(z) \tag{22}$$

$$K_c(z) = K_d(z) = K_2(z) \tag{23}$$

In the ring-core strain rosette three strain gages exist, therefore, $d\varepsilon_d$ in Eq. (21) could be written as a function of the three other variables.

$$d\varepsilon_d = d\varepsilon_a - d\varepsilon_b + d\varepsilon_c \tag{24}$$

By combining the Eqs. (16) to (24), the stress in the direction of the three strain gage would be calculated by Eqs. (25) to (27).

$$\sigma_a(z) = \frac{E}{K_1^2 - \nu^2 K_2^2}\left[K_1(z)\frac{d\varepsilon_a(z)}{dz} + \upsilon K_2(z)\frac{d\varepsilon_c(z)}{dz}\right] \tag{25}$$

$$\sigma_b(z) = \frac{E}{K_1^2 - \nu^2 K_2^2}\left[\begin{array}{l} K_1(z)\dfrac{d\varepsilon_b(z)}{dz} \\ +\upsilon K_2(z)\left(\dfrac{d\varepsilon_a(z)}{dz} - \dfrac{d\varepsilon_b(z)}{dz} + \dfrac{d\varepsilon_c(z)}{dz}\right)\end{array}\right] \tag{26}$$

$$\sigma_c(z) = \frac{E}{K_1^2 - \nu^2 K_2^2}\left[K_1(z)\frac{d\varepsilon_c(z)}{dz} + \upsilon K_2(z)\frac{d\varepsilon_a(z)}{dz}\right] \tag{27}$$

In the ring-core strain rosette, each gage is displaced by 45 degrees. Therefore, two strain gages are perpendicular. It is considered that “a” and “c” are perpendicular and “b” is in 45 degrees in a counter-clock wise direction respect to the “a”. A typical Mohr’s circle related to the ring-core strain rosette is indicated in Fig. 3. By attention to Fig. 3 the principal residual stresses and also direction between the gages “a” and the maximum principal residual stress are measured by Eqs. (28) and (29).

$$\sigma_{1,2}(z) = \frac{\sigma_a(z) + \sigma_c(z)}{2} \pm \frac{1}{2}\sqrt{2}\sqrt{\left[\sigma_b(z) - \sigma_a(z)\right]^2 + \left[\sigma_b(z) - \sigma_c(z)\right]^2} \tag{28}$$

$$\varnothing = \frac{1}{2} arc\tan\frac{2\sigma_b(z) - \sigma_a(z) - \sigma_c(z)}{\sigma_a(z) - \sigma_c(z)} \tag{29}$$

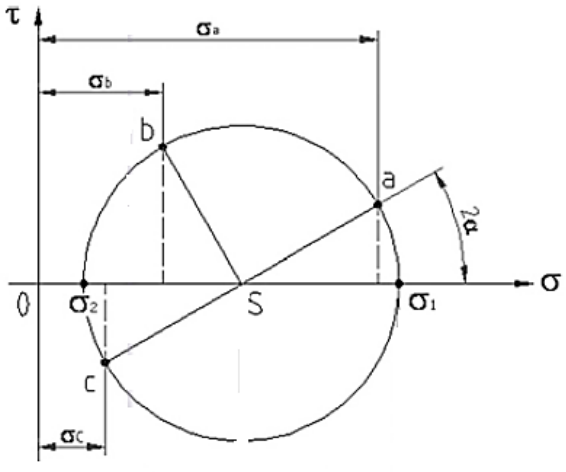

Fig. 3. Mohr’s circle related to the ring-core strain rosette.

3- Determination of the Calibration Constants

If the elastic constant of the material, E and υ and also the calibration coefficients $K_1(Z)$ and $K_2(Z)$ are known, the residual stresses could be calculated by the Eqs. (25) to (29). Therefore, determination the calibration coefficients are a pre-required step for experimental test.

The calibration coefficients of the incremental method are determined by the Eqs. (10) and (11). In the calibration coefficient determination process, a known field of stress shall be used. It is possible to determine the calibration coefficients by experimental method and tension or compression test, but in real material always a value of residual stresses exist and could effect on the final value. Therefore, the finite element method is known as an appropriate way to determine the calibration constants.

In this research the ABAQUS finite element package has been used to determine the calibration coefficient of the incremental method. The dimension of the finite element model considered as 50×50×25 mm. Due to the symmetry, only a quarter of the model has been modeled (25×25×25 mm) and indicated in Fig. 4.

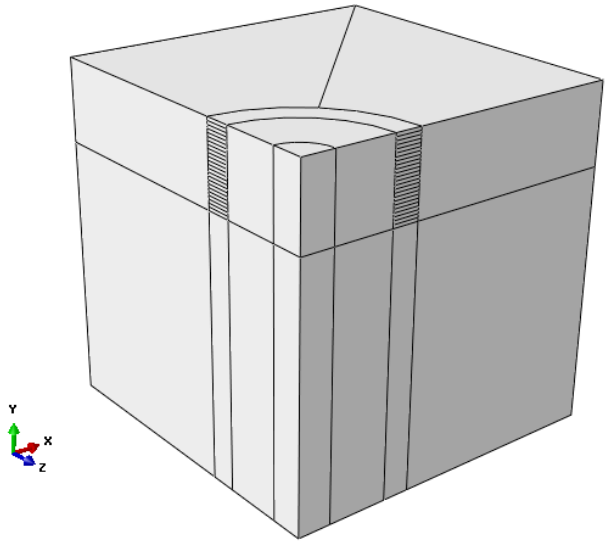

Fig. 4. Finite element model of the ring-core calibration.

The material is considered as linear elastic and isotropic and the annular groove has been modeled in 20 equal increments with the size of ΔZ= 0.25mm. Parameter of the finite element model indicated in the Table 1.

In the position of the strain rosette the fine mesh has been used. The mesh sizing study indicated that appropriate dimension for the mesh of the strain rosette portion is about 0.7 mm. Figs. 5 and 6 present the model after first and final

Table 1. Parameters of the FEM

parameters	Value
Dimension (mm)	25 × 25 × 25
Annular groove (mm)	Ø14-Ø18
Elasticity modulus (GPa)	200
Poison ratio	0.3
Uniaxial stress (MPa)	50
Element type	C3D20
Gage length of strain rosette (mm)	5

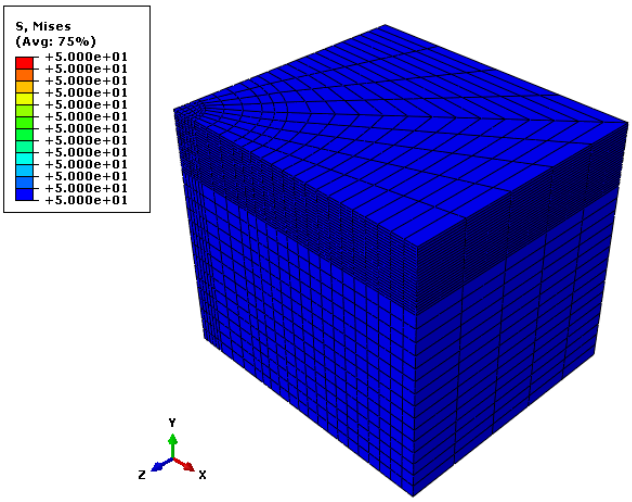

Fig. 5. Model at the end of the first step.

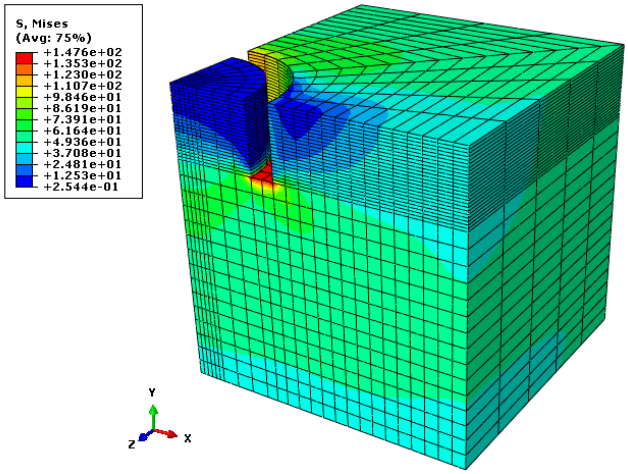

Fig. 6. Model at the end of the final step.

steps, respectively.

Stress contours indicate that, increase in the depth of the annular groove result to stress release in the core. To calculate the calibration coefficients, the strain values in principal directions have been measured. Fig. 7 indicates the released strain in the principal directions.

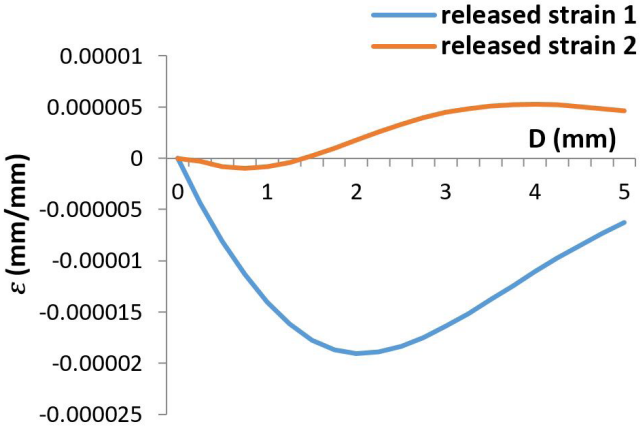

Fig. 7. Released strain in principal directions in term of the annular groove depth.

The calibration factors have been calculated by Eqs. (10) and (11), and the results have been indicated in Fig. 8.

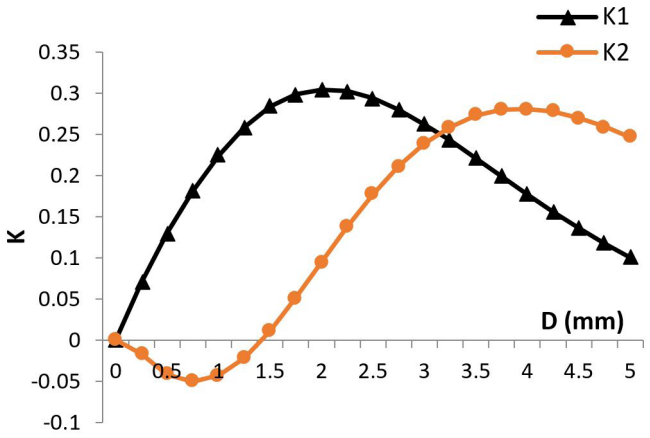

Fig. 8. Calibration coefficients in term of the annular groove depth.

The data in Fig. 8 have been obtained from the simulation of the tension test. In theory, it is possible to use the compression stress too. To compare the results between tension and compression stress, the calibration process has been done under 50 MPa compression stress. The released strains in principal directions have been indicated in Fig. 9, but the final results are exactly the same as data in Fig. 8.

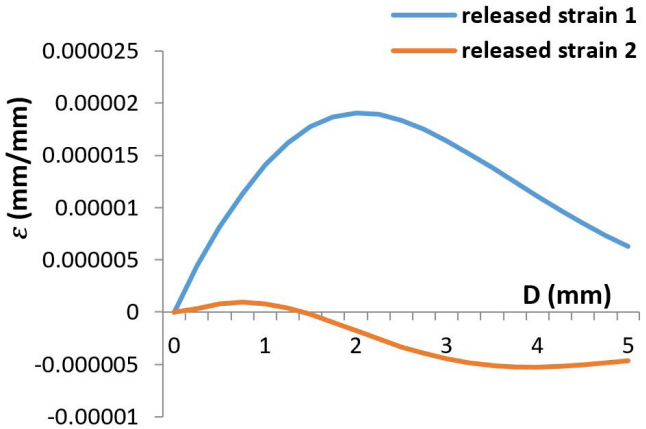

Fig. 9. Released strain in principal directions in term of the annular groove depth in the compression test.

The calibration constant should be unique and different loading condition should not affect them. In case of the biaxial stress the calibration coefficient could be calculated by Eqs. (30) and (31).

$$K_1(Z)=\left(\frac{E\sigma_2}{\sigma_2^2-\sigma_1^2}\right)\left(\frac{d\varepsilon_2(Z)}{dz}\right)+\left(\frac{d\varepsilon_1(Z)}{dz}\right)\left(\frac{E}{\sigma_1}\right)\left(1-\frac{\sigma_2^2}{\sigma_2^2-\sigma_1^2}\right) \quad (30)$$

$$K_2(Z)=\left(\frac{E\sigma_1}{\nu(\sigma_2^2-\sigma_1^2)}\right)\left(\frac{d\varepsilon_2(Z)}{dz}-\frac{d\varepsilon_2(Z)}{dz}\left(\frac{\sigma_2}{\sigma_1}\right)\right) \quad (31)$$

The calibration process in the biaxial condition has been simulated by σ_1=80 MPa,and σ_2=50 MPa and released strains in the principal directions have been indicated in Fig. 10. The calibration constants have been calculated by Eqs. (30) and (31) and the results have been indicated in Fig. 11.

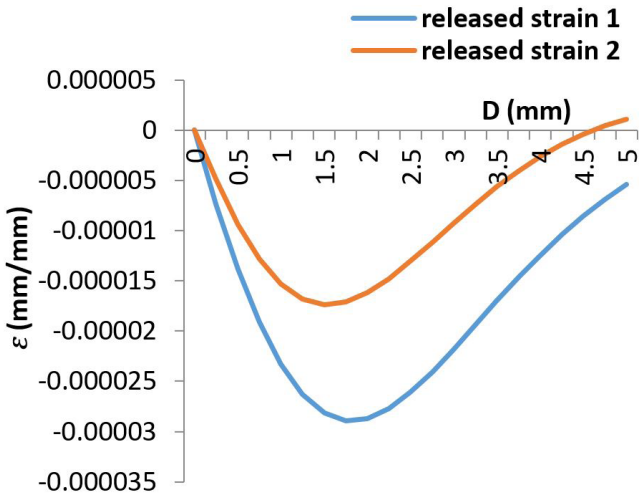

Fig. 10. Released strain in principal directions in term of the annular groove depth in the biaxial test.

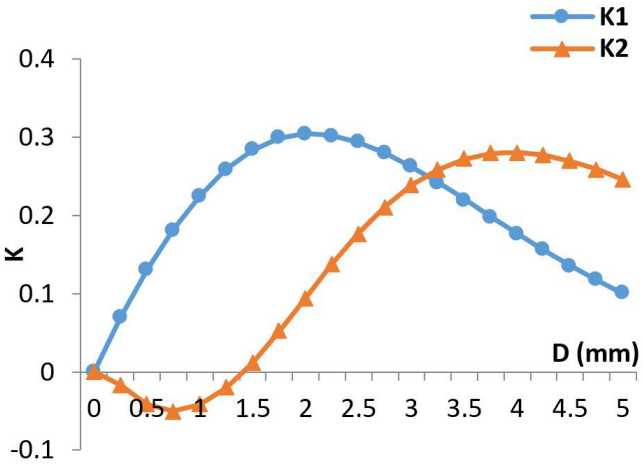

Fig. 11. Calibration coefficients in term of the annular groove depth.

4- Verification of the Calibration Coefficients

The calibration coefficients are valuable if they be verified. To verify the calibration coefficient, it is possible to use the experimental test as well as the finite element method. Similar to the determination of the calibration coefficient several parameters such as residual stresses exist in experimental tests that could effect on the final results. To prevent the unexpected problems, the finite element method has been used for verification the calibration constants.

In a first step the uniform residual stresses have been simulated. Parameters of the model are similar to what explained in the previous section. The uniaxial tensile stress with σ_1=50 MPa,and σ_2=0 have been considered. The released strains in the directions of the strain rosette (Fig. 2) have been measured and indicated Fig. 12. Several models with different dimensions have been used, but, there was not any significant change in the results. Simulation consists of 21 steps. In the first step the loading is simulated and in the next 20 steps the depth of the annular groove increased by ΔZ= 0.25mm.

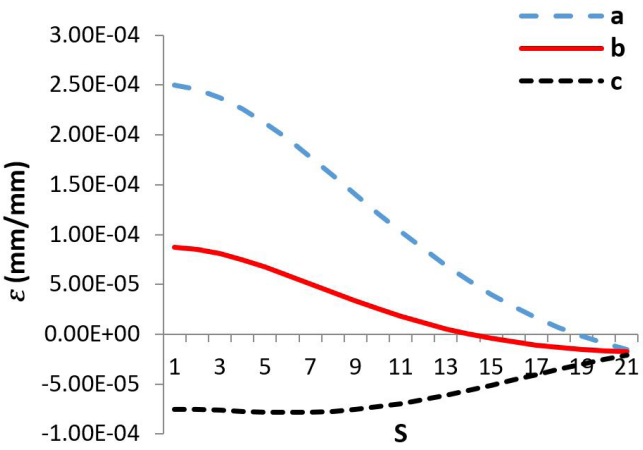

Fig. 12. Released strain in strain rosette directions, in term of the simulation steps (at each step the depth of annular grooves increase by 0.25mm).

The residual stresses corresponding to the directions of the strain rosette have been calculated by Eqs. (25) to (27) and the calibration constants. The results have been indicated in Fig. 13.

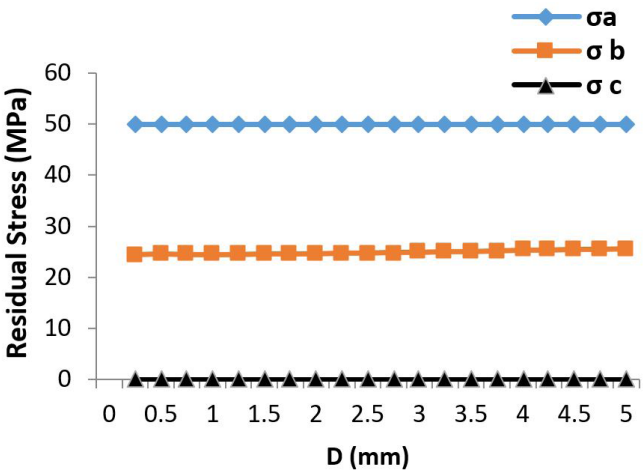

Fig. 13. Calculated residual stresses in strain rosette directions, in term of the annular groove depth.

The principal residual stresses have been calculated by Eq. (28) and indicated in Fig. 14.

The angle between the gages “a” and the maximum principal residual stress have been calculated by Eq. (29) and indicated in Fig. 15.

In the uniform case of the residual stresses, the biaxial condition has been considered by σ_1=80 MPa,and σ_2=50 MPa. All of the model parameters except the loading condition were similar to the uniaxial condition. The released strains and appropriate residual stresses in strain rosette directions have been indicated in Figs. 16 and 17.

The principal residual stresses and also the angle between the gage “a” and the maximum principal residual stresses have been indicated in Fig. 18 and 19.

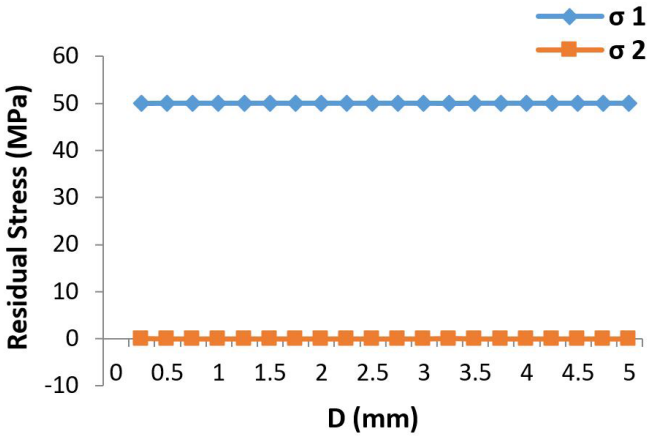

Fig. 14. Calculated principal residual stresses in term of the annular groove depth.

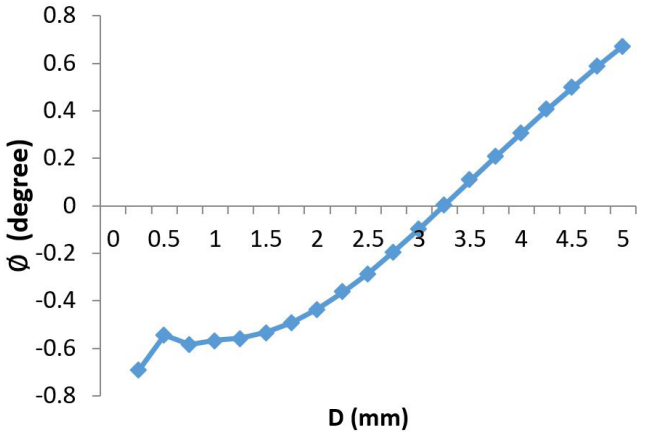

Fig. 15. Angle between the gage "a" and the maximum principal residual stress in term of the annular groove depth.

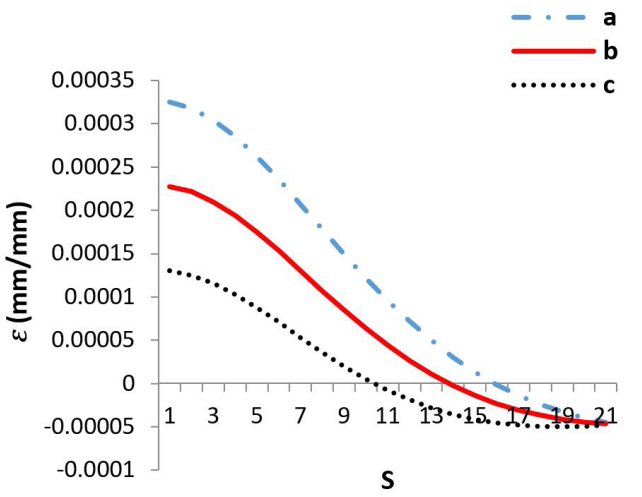

Fig. 16. Released strain in strain rosette directions, in term of the simulation steps (in each step the depth of annular groove increase by 0.25mm) of the biaxial case.

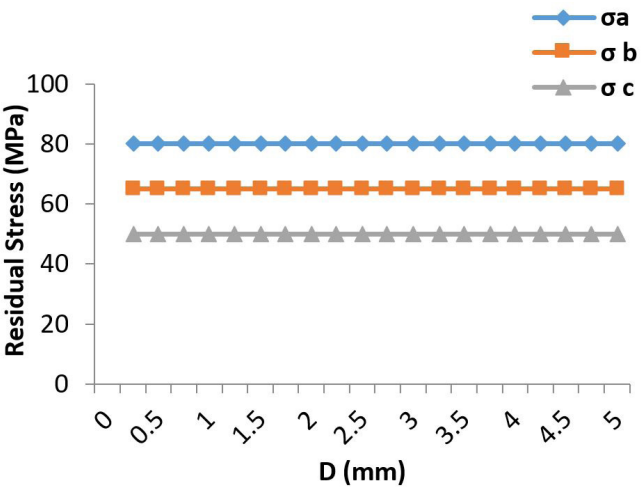

Fig. 17. Calculated residual stresses in strain rosette directions, in term of the annular groove depth- The biaxial case.

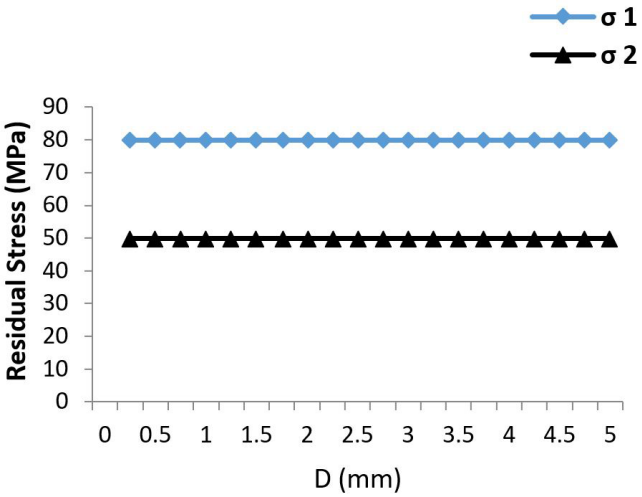

Fig. 18. Calculated principal residual stresses in term of the annular groove depth- The biaxial case.

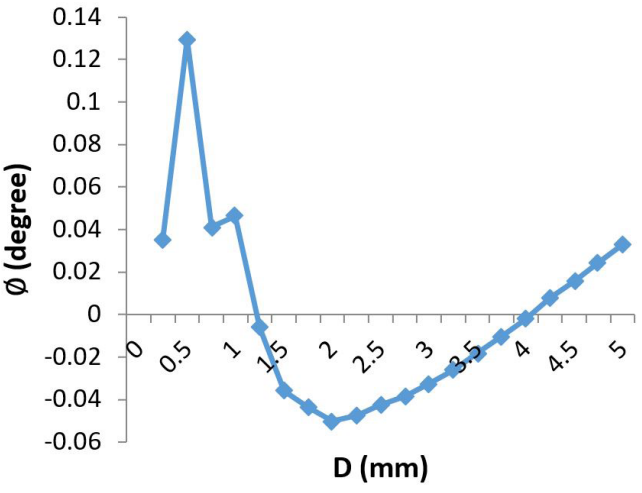

Fig. 19. Angle between the gage "a" and the maximum principal residual stress in term of the annular groove depth- The biaxial case.

Addition to the uniform cases of the residual stresses, the uniaxial non-uniform case has been considered. The only change in the model was the loading. After simulation and extracting the data, the principal residual stresses and also the actual applied stresses along the gage "a" that is the loading direction, have been calculated and indicated in Fig. 20. The angle between the maximum principal residual stresses and the gage "a" has been indicated in Fig. 21.

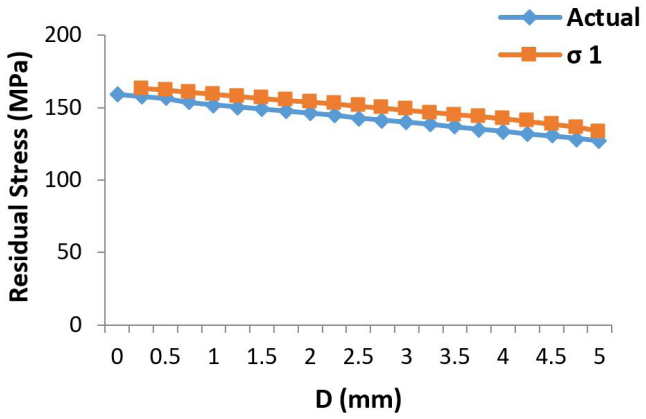

Fig. 20. The maximum principal residual stresses and applied stresses in term of the annular groove depth- The non-uniform uniaxial case.

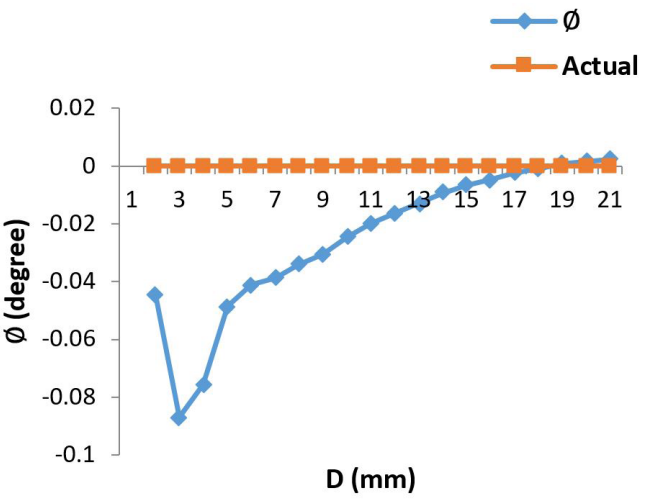

Fig. 21. Angle between the gage "a" and the maximum principal residual stress in term of the annular groove depth-The non-uniform uniaxial case.

5- Experimental Test

To verify the calibration constant an experimental test has been devised. In this test a plate is subjected to the uniaxial tension condition and then the ring-core method is used to measure the applied stress. Devised fixture, specimen, special cutter for mashing the annular groove and strain rosette for the ring-core method are indicated in Fig. 22.

The fixture is made from a piece of rail and after machining process heat treated to obtain 45 HRC hardness. The specimen is made of mild steel (S235JR EN 10025). The specimen have been annealed after machining and just slightly polished to make a clean surface.

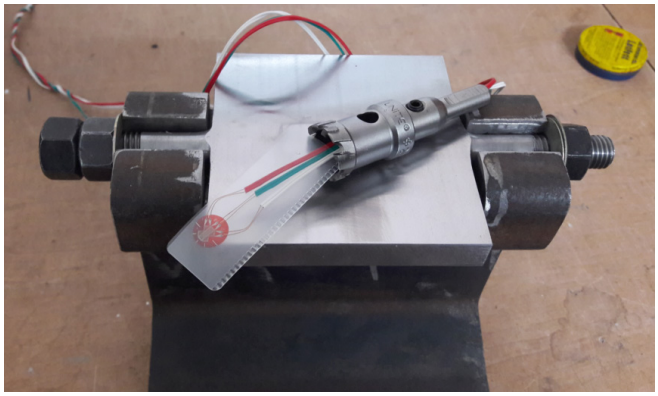

Fig. 22. Devised fixture, specimen, cutter and rosette for experimental test

The fixture is considered as a rigid body in comparing with the specimen. The specimen has been subjected to tensile stress by fasten the nuts. The value of tensile strains has been controlled by the strain gage which bonded along the direction of the applied strain. Then the ring-core process has been done in 20 equivalent steps (each depth step=0.25mm). Different parameters of the test have been indicated in the Table 2 and the test setup is indicated in Fig. 23.

Table 2. Parameters of the Experimental test

parameters	Value
Dimension of the specimen (mm)	100 × 100 × 15
Elasticity modulus (GPa)	200
Poison's ratio	0.3
Uniaxial Applied strain	86e-6
Uniaxial stress (MPa)	17.2
Strain rosette	TML-FRA-5-11
Annular groove (mm)	Ø14-Ø18
Depth step (mm)	0.25
Final depth (mm)	5

After machining the annular groove and record the relived strain in each step, the value of the stresses has been calculated according to the procedure of the ring-core method. The relived strains after filtering the noises have been indicated in Fig. 24. To calculate the stresses the calibration coefficients which obtained from the FE analysis have been used and Fig. 25 shows the results.

By attention to the test condition it is possible to calculate the calibration coefficients by using the data of Fig. 24 and Eqs. (10) and (11). The calculated calibration constant and also, the calibration constant by FE analysis have been indicated in the Fig. 26.

6- Conclusions

This paper offers some information about the residual stress measurement by semi-destructive ring-core method. The basic formulas have been presented and a procedure for determining the calibration coefficient for certain material has been introduced.

The calibration coefficients have been determined by simulation the uniaxial tension and compression tests. Also the required formula to determine the calibration constants

Fig. 23. Setup of the experimental test

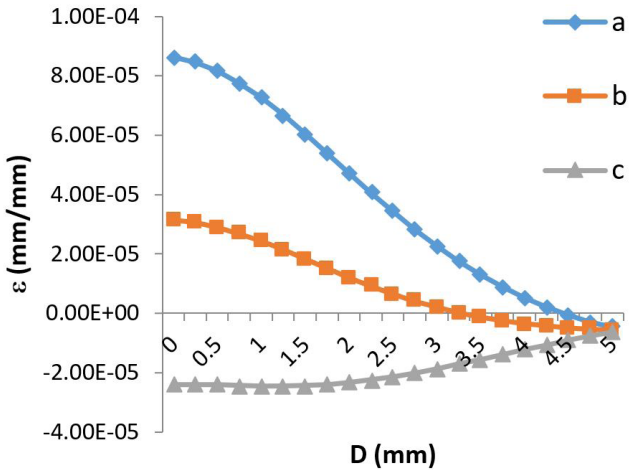

Fig. 24. Recorded strains in rosette in term of the annular groove depth

in the biaxial case have been introduced. It is indicated that the calibration constants in uniaxial and biaxial conditions are the same. The calibration constants of both uniaxial and biaxial conditions have been indicated in the Table 3. This point shows that the calibration coefficients are independent of loading directions.

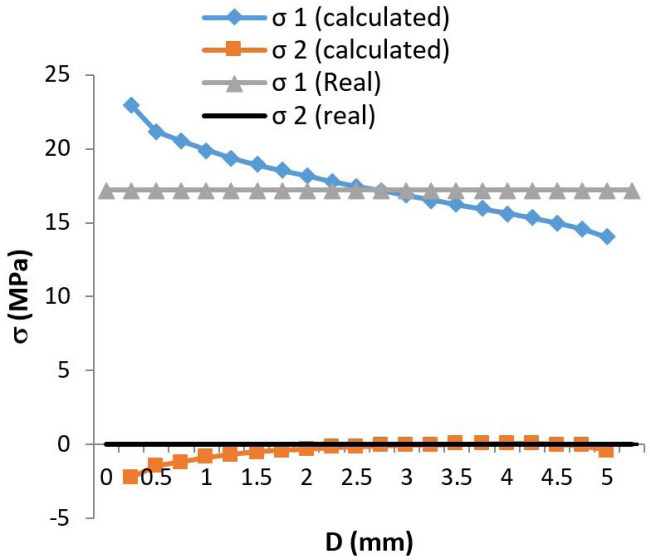

Fig. 25. Calculated principal residual stresses by the ring-core method and real applied stresses in the experimental test

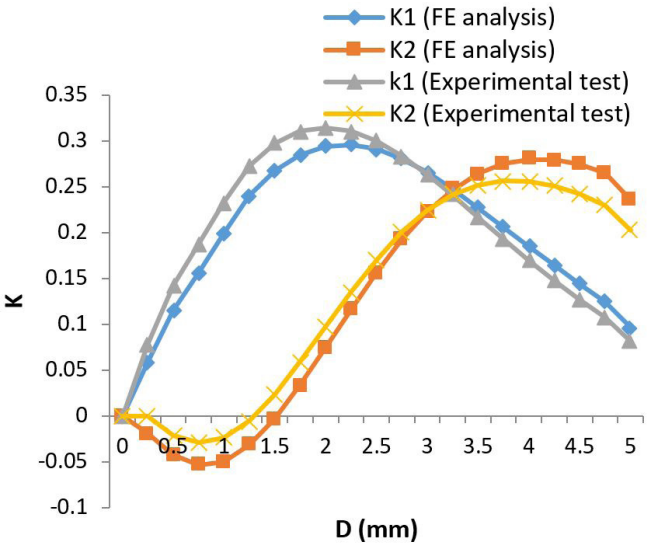

Fig. 26. Calibration constants by FE analysis and experimental test

The calibration constants have been verified by simulation the uniform and non-uniform cases of the residual stresses. In the case of the uniform residual stresses, it is indicated that the introduced formula and calibration coefficient could calculate the residual stress field. The conformity between the applied stress in finite element analysis and calculated stress was about 100%. Also the direction between the maximum principal residual stresses and gage "a" have been calculated by a clearance about ±0.7° that is excellent. The non-uniform case of residual stresses also have been considered and indicated that the maximum difference between the applied and calculated residual stresses was about 1% that is very good.

An experimental test has been devised to show the effectiveness the calculated calibration constant. In this test a uniform case of stresses is formed by creating uniaxial tensile strains in a plate. Comparing the calculated and applied

Table 3. the calibration constants in uniaxial and biaxal conditions

depth (mm)	K_1 uniaxial	K_2 uniaxial	K_1 biaxial	K_2 biaxial
0	0	0	0	0
0.25	0.069904	-0.016816	0.069930256	-0.016478632
0.5	0.130288	-0.042037333	0.130373333	-0.041688889
0.75	0.18128	-0.0504	0.18137641	-0.049832479
1	0.224944	-0.042864	0.225071795	-0.042070427
1.25	0.259248	-0.021232	0.259364103	-0.02045812
1.5	0.283872	0.011573333	0.283944615	0.012131282
1.75	0.2988	0.051616	0.298838974	0.052047863
2	0.304704	0.094896	0.304710769	0.095150769
2.25	0.302688	0.137781333	0.30266441	0.137890188
2.5	0.294016	0.177344	0.293952513	0.177240068
2.75	0.2801392	0.211488	0.280059385	0.211255385
3	0.2624704	0.239018667	0.262373744	0.238665299
3.25	0.2423088	0.259466667	0.242205949	0.25902906
3.5	0.2207728	0.272933333	0.220673641	0.272456752
3.75	0.1987808	0.279936	0.198686687	0.279450598
4	0.177032	0.281237333	0.176946133	0.280751111
4.25	0.15604512	0.277701333	0.155972103	0.277248547
4.5	0.13617104	0.270218667	0.13611159	0.269805812
4.75	0.11763104	0.259626667	0.117582769	0.259257436
5	0.1005448	0.246698667	0.100506872	0.24637265

stresses shows that the results of the ring-core method are acceptable.

The calculated calibration constant by experimental test shows a similar trend by the results of the FE analysis. This note confirms the FE analysis, but small variation in calibration constant cause to big mistakes in calculating stresses. Moreover, in experimental test several uncertainty effects on the results which are not controllable. Therefore the authors just present the FE analysis values. By attention to the results it is concluded that the presented calibration coefficients have enough accuracy to use as the pre-required constant in the incremental ring-core method

References

[1] European Standard, prEN 13674-1, Railway Applications-Track-Rail, Part 1: Vignole railway rails 46 kg/m and above, Nov. 2002.

[2] M. Sedighi, M. Honarpisheh, Experimental study of through-depth residual stress in explosive welded Al–Cu–Al multilayer, *Materials & Design,* 37 (2012) 577-581.

[3] M. Sedighi, M. Honarpisheh, Investigation of cold rolling influence on near surface residual stress distribution in explosive welded multilayer, *Strength of Materials,* 44(6) (2012), 693-698.

[4] M. Honarpisheh, E. Haghighat, M. Kotobi, Investigation of residual stress and mechanical properties of equal channel angular rolled St12 strips, Proceedings of the Institution of Mechanical Engineers, *Part L: Journal of Materials: Design and Applications* (2016) https://doi.org/10.1177/1464420716652436.

[5] M. Kotobi, M. Honarpisheh, Uncertainty analysis of residual stresses measured by slitting method in equal-channel angular rolled Al-1060 strips, *The Journal of Strain Analysis for Engineering Design,* 52(2) (2017), 83-92.

[6] M. Kotobi, M. Honarpisheh, Experimental and numerical investigation of through-thickness residual stress of laser-bent Ti samples, *The Journal of Strain Analysis for Engineering Design,* 52(6) (2017) 347-355.

[7] M. Kotobi, M. Honarpisheh,Through-depth residual stress measurement of laser bent steel–titanium bimetal sheets, *The Journal of Strain Analysis for Engineering Design,* 53(3) (2018) 130-140.

[8] I. Alinaghian, M. Honarpisheh, S. Amini, The influence of bending mode ultrasonic-assisted friction stir welding of Al-6061-T6 alloy on residual stress, welding force and macrostructure, *The International Journal of Advanced Manufacturing Technology,* 95 (5-8) (2018) 2757-2766.

[9] I. Alinaghian, S. Amini, M. Honarpisheh, Residual stress, tensile strength, and macrostructure investigations on ultrasonic assisted friction stir welding of AA 6061-T6, *The Journal of Strain Analysis for Engineering Design,* 53(7) (2018) 494-503.

[10] ASTM E837 − 13a. *Standard Test Method for Determining Residual Stresses by the Hole-Drilling Strain-Gage Method*, (2013).

[11] M. Barsanti, M. Beghini,C. Santus, A. Benincasa,L. Bertelli, Integral method coefficients and regularization

procedure for the ring-core residual stress measurement technique, *Advanced Materials Research,* 996 (2014) 331-336.

[12] M. A. Moazam, M. Honarpisheh, Residual Stresses Measurement in UIC 60 Rail by Ring-Core Method and Sectioning Technique, *AUT J. Mech. Eng.*, 2(1) (2017) 99-106.

[13] F. Mendaa, P. Šarga, T. Lipták, F. Trebuna, Comparison of different simulation approaches in ring-core method, *American Journal of Mechanical Engineering,* 2(7) (2014) 258-261.

[14] A. Misra, H. A. Peterson, Examination of the ring method for determination of residual stresses, *Experimental Mechanics,* 21(7) (1981) 268-272.

[15] S. Keil, Experimental determination of residual stresses with the ring-core method and an on line measuring, *Experimental Technique,* 16(5) (1992) 17-24.

[16] J. Vaclavik, O. Weinberg, P. Bohdan, J. Jankovec and S. Holy, Evaluation of Residual Stresses using Ring Core Method, 14th *International Conference on Experimental Mechanics,* (2010) 1-10.

[17] A. Civin, M. Vlk, Analysis of Calibration Coefficients for Incremental Strain Method Used for Residual Stress Measurement by Ring-Core Method, *Applied Mechanics,* (2010) 25–28.

[18] K.P. Milbradt, *Ring-method Determination of Residual Stresses*, Proc. SESA Sw'ng Meeting, Cleveland (1950) 63- 74.

[19] Tokyo Sokki KenkyujoCo, Ltd., TML Strain gage cataloge, Accessed on 1 Aguest 2016; http://www.tml.jp/e.

[20] A. Civin, M. Vlk, Determination of principal residual stresses' directions by incremental strain method, *Applied and Computational Mechanics,* 5 (2011) 5–14.

[21] A. Ajovalasit, G. Petrucci,B. Zuccarello, Determination of nonuniform residual stresses using the Ring-Core method, *Journal of Engineering Materials and Technology,* 118(2) (1996) 224-228.

[22] M. Barsanti, M. Beghini, C. Santus, A. Benincasa, L. Bertelli, Integral method coefficients for the ring-core technique to evaluate non-uniform residual stresses, *The Journal of Strain Analysis for Engineering Design,* 53(4) (2018) 210-224.

Please cite this article using:

M. A. Moazam and M. Honarpisheh, Experimental and Numerical Study on the Accuracy of Residual Stress Measurement by Incremental Ring-Core Method, *AUT J. Mech. Eng.*, 2(2) (2018) 137-148.

DOI: 10.22060/ajme.2018.13954.5697